Table VI. Sodium and Water Coordination Distances in $Na_4[(VO)_2((+)\text{-mmt})((-)\text{-mmt})]\cdot 14H_2O$[a]

Na(1)-O(4)	2.448 (5)	Na(2)-O(1)	2.352 (4)
-O(3)	2.480 (4)	-O(9)	2.461 (5)
-O(8)	2.358 (4)	-O(12)	2.457 (5)
-O(10)	2.397 (5)	-O(13)	2.539 (5)
-O(12)	2.429 (6)	-O(14A)	2.544 (11)
-O(10)[b]	2.398 (4)	-O(14B)	2.192 (10)
		-O(13)[c]	2.480 (6)
O(8)-O(8)[d]	2.777 (11)	O(11)←O(14A)	2.554 (17)
O(8)→O(6)[e]	2.780 (5)	O(11)←O(14B)	2.986 (17)
O(8)←O(13)[f]	2.856 (5)	O(12)→O(7)[h]	3.044 (7)
O(9)←O(11)[g]	2.747 (5)	O(12)→O(2)[i]	2.884 (7)
O(9)→O(1)[c]	2.827 (5)	O(13)→O(5)[j]	2.722 (5)
O(9)→O(7)[h]	2.787 (5)	O(14A)-O(14A)[g]	3.15 (3)
O(10)→O(11)	2.797 (5)	O(14A)→O(2)[f]	2.832 (15)
O(10)→O(2)[i]	2.832 (5)	O(14B)-O(14B)[g]	2.74 (3)
		O(14B)→O(2)	3.189 (15)

[a] The arrows indicate hydrogen atom donor-acceptor relationships between hydrogen bonded oxygen atoms. [b] $1-x,-y,-z$. [c] $1-x,1-y,1-z$. [d] $1-x,1-y,-z$. [e] $-x,1-y,-z$. [f] $x,y,1+z$. [g] $1-x,y,z$. [h] $1+x,y,z$. [i] $1-x,-y,-z$. [j] $x,1-y,1-z$.

is most likely due to variations between the structures in the 77 K glass, in which the ESR studies were conducted, and in the crystal. That this is the case is indicated by our calculation of a zero-field splitting parameter D for the crystalline material of -0.0279 cm^{-1} from the V-V′ distance of 4.047 Å, the measured isotropic g value (solution) of 1.964, and the angle between the V=O and V—V′ vectors (θ) of 24.70° (assumed equal to the angle between the interelectron vector R and the magnetic quantization axis) using equations in ref 3. This value is in excellent agreement with the value of $|D| \approx 0.028$ cm^{-1} estimated from the powder ESR spectrum of the tetradecahydrate.[3] Thus, not only is the D value different for the crystal and the glass, but the crystal value can be calculated from the geometrical parameters determined in the crystal structure.

Crystal Packing. Water molecules and oxygen atoms of the tetranegative anion form octahedral coordination polyhedra around the two crystallographically independent sodium ions. Table VI lists the coordination distances for the sodium ions and the hydrogen-bonded water molecule, and Figure 2 shows the contents of the unit cell. As mentioned earlier, O(14) is disordered with a similar coordination about both positions though the Na(2)–O(14B) distance of 2.192 Å is very short. The final difference map indicates hydrogen disorders involving the hydrogen donor–acceptor relationships between O(8) and another atom related by a center of symmetry. A similar disorder may be present with O(14A) and O(14B) where water molecule oxygen atoms also related by a center of symmetry are coordinated. The difference peaks observed about O(8), O(14A), and O(14B) were not well resolved, and the disorder was not probed further.

Acknowledgment. This work was supported by grants from the Minority Biomedical Sciences Program (NIH-DRR No. 506 RR08139), the National Science Foundation (No. CH-780921) for purchase of the Syntex P3/F and R3 diffractometer and computing systems, and the University of New Mexico for the use of the IBM 360/67/65 computers and for a faculty grant through the Research Allocations Committee. Dr. Eileen Duesler aided in the preparation of computer-generated figures.

Registry No. $Na_4[(VO)_2((+)\text{-mmt})((-)\text{-mmt})]\cdot 14H_2O$, 79854-25-4.

Supplementary Material Available: Listings of idealized hydrogen atom positions and observed and calculated structure factors (22 pages). Ordering information is given on any current masthead page.

Contribution from the Department of Chemistry, Baker Laboratory, Cornell University, Ithaca, New York 14853

Dioxygenase Models. Crystal Structures of [*N*,*N*′-(1,2-Phenylene)bis(salicylideniminato)](catecholato-*O*)iron(III) and μ-(1,4-Benzenediolato-*O*,*O*′)-bis[*N*,*N*′-ethylenebis(salicylideniminato)iron(III)]

ROBERT H. HEISTAND, II, A. LAWRENCE ROE, and LAWRENCE QUE, JR.*

Received July 9, 1981

Two iron phenolate complexes have been synthesized to serve as models for dioxygenase enzyme–substrate and enzyme–inhibitor interactions; their X-ray structures have been determined. Fe(saloph)catH, a monodentate catecholate complex, crystallizes in the triclinic space group $P\bar{1}$ (a = 9.960 (6) Å, b = 8.108 (3) Å, c = 13.849 (8) Å, α = 95.73 (4)°, β = 91.93 (5)°, γ = 72.13 (4)°), while $[Fe(salen)]_2hq$, a bridged hydroquinone complex, crystallizes in the orthorhombic space group *Pbca* (a = 12.917 (3) Å, b 13.100 (4) Å, c = 19.440 (4) Å, $\alpha = \beta = \gamma = 90°$). The irons in both complexes exhibit properties typical of square-pyramidal geometry—metal atom raised above the basal mean plane (0.55 Å for Fe(saloph)catH and 0.50 Å for $[Fe(salen)]_2hq$) and short apical Fe–O bonds (1.828 (4) Å for Fe(saloph)catH and 1.861 (2) Å for $[Fe(salen)]_2hq$). The average Fe–O and Fe–N bond lengths in the two tetradentate ligands are the same in both structures (1.905 and 2.079 Å, respectively) and are in excellent agreement with those found for similar complexes. Fe(saloph)catH and $[Fe(salen)]_2hq$ represent the first monodentate catecholate and the first bridged hydroquinone structures, respectively, of iron(III).

Introduction

The active-site structure and the reaction mechanism of the catechol-cleaving dioxygenases have been the subject of many investigations in recent years.[1,2] The active sites of these enzymes have been demonstrated to consist of mononuclear high-spin ferric centers[3,4] coordinated to two tyrosinates.[5,6] Other coordinating groups are not known at present, though nitrogen[3] and sulfur[7] donors have been suggested. Catechols

(1) Nozaki, M. In "Molecular Mechanisms of Oxygen Activation"; Hayaishi, O., Ed.; Academic Press: New York, 1974; Chapter 4.
(2) Que, L., Jr. *Struct. Bonding (Berlin)* **1980**, *40*, 39-72.
(3) Que, L., Jr.; Lipscomb, J. D.; Zimmermann, R.; Munck, E.; Orme-Johnson, W. H.; Orme-Johnson, N. R. *Biochim. Biophys. Acta* **1976**, *452*, 320-334.
(4) Kent, T.; Munck, E.; Widom, J.; Que, L., Jr., unpublished results.
(5) Que, L., Jr.; Heistand, R. H., II; Mayer, R.; Roe, A. L. *Biochemistry* **1980**, *19*, 2588-2593.
(6) Que, L., Jr.; Epstein, R. M. *Biochemistry* **1981**, *20*, 2545-2549.

0020-1669/82/1321-0676$01.25/0

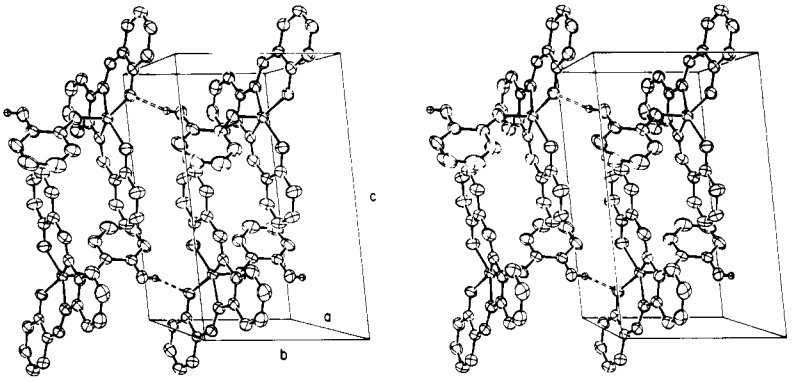

Figure 1. Packing diagram of Fe(saloph)catH viewed down the *a* axis. Note the hydrogen bond indicated by a dashed line.

bind to the active-site iron, altering the visible spectrum, and resonance Raman spectra are consistent with a chelated configuration.[7,8] However, steady-state inhibition kinetic studies with *m*- and *p*-hydroxybenzoates on protocatechuate 3,4-dioxygenase suggest that the ferric center coordinates only to the *p*-hydroxy function,[9] and this has been confirmed by resonance Raman evidence.[6] Thus, the nature of the enzyme–substrate interaction remains unclear.

We have proposed an enzyme mechanism where a monodentate catecholate–iron complex is suggested as the enzyme–substrate complex.[9] However, no examples of such complexes have been reported prior to our work, though examples of chelated structures abound.[10] Recently, we reported on the reactivity of one such monodentate complex with oxygen and the corresponding lack of reactivity of a closely related chelated complex.[11] In this paper, we report the crystal structure of Fe(saloph)catH,[12] an iron complex with monodentate catecholate coordination, as well as that of a hydroquinone complex $[Fe(salen)]_2hq$.[13,14] Both these structures are the first of their kind to be reported, and the complexes serve as models for enzyme–substrate and enzyme–inhibitor interactions in the dioxygenases.

Experimental Section

Synthesis. All reactions were performed under an atmosphere of purified, dried nitrogen in Schlenk apparatus. Reagent acetonitrile (Burdick and Jackson) was trap to trap distilled from NaH under reduced pressure. Ethyl acetate was dried over 3-Å sieves. Hydroquinone and catechol were sublimed.

Fe(saloph)catH. A solution (300 mL, 3.36 mM) of Fe(saloph)OAc[15,16] in dry acetonitrile was degassed in vacuo, heated to reflux, and filtered to remove $[Fe(saloph)]_2O$. To the hot filtrate was added a degassed, hot solution of catechol (15 mL, 0.67 M) in ethyl acetate via a cannular tube. Upon slow overnight cooling, long black hexagonal plates crystallized from the solution. Vacuum filtration and washing with ethyl acetate yielded 0.35 g (73%) of Fe(saloph)catH. Anal. Calcd for $C_{16}H_{19}FeN_2O_4$: C, 65.16; H, 4.00; N, 5.84. Found: C, 65.13; H, 4.16; N, 5.92.

$[Fe(salen)]_2hq$. A degassed solution of 35 mL (28.6 mM) of Fe(salen)OAc[15,16] in reagent acetonitrile was heated to reflux and filtered. To the hot filtrate was added a degassed, hot solution of hydroquinone (35 mL, 1.45 M) in ethyl acetate. Upon slow cooling, large 2-mm cubes crystallized after 2 days; filtration and washing with ethyl acetate yielded 0.37 g (84%) of $[Fe(salen)]_2hq$. Anal. Calcd for $C_{38}H_{32}N_4Fe_2O_6$: C, 60.66, H, 4.29; N, 7.45. Found: C, 60.66; H, 4.57; N, 7.46. A previously reported synthesis of $[Fe(salen)]_2hq$ from Fe(salen) and *p*-benzoquinone yielded a microcrystalline powder.[13,14]

Table I. Crystallographic Data

	Fe(saloph)catH	$[Fe(salen)]_2hq$
formula	$C_{26}H_{19}FeN_2O_4$	$C_{38}H_{32}Fe_2N_4O_6$
mol wt	479.30	752.39
space group	$P\bar{1}$	*Pbca*
a, Å	9.960 (6)	12.917 (3)
b, Å	8.108 (3)	13.100 (4)
c, Å	13.849 (8)	19.440 (4)
α, deg	95.73 (4)	90.0
β, deg	91.93 (5)	90.0
γ, deg	72.13 (4)	90.0
V, Å^3	1059 (1)	3290 (1)
Z	2	4
D_m, g/cm^3	1.497 (5)	1.518 (3)
D_{calcd}, g/cm^3	1.502	1.519
radiation used	Cu K$\bar{\alpha}$ (λ = 1.5418)	Mo K$\bar{\alpha}$ (λ = 0.71069)
max ($\sin\theta/\lambda$)	0.54	0.60
crystal size, mm	0.50 × 0.10 × 0.025	0.28 × 0.30 × 0.43
μ, cm^{-1}	6.150	0.965
no. of reflctns measd	2797	3287
data used [$\lvert F\rvert = 3(\sigma(F))$]	2534	2536
no. of variables used	298	275
R	0.076	0.043
R_w	0.092	0.072
goodness of fit[a]	0.420	0.273

[a] GOF = $[\Sigma w(F_o - kF_c)^2/(N_{obsd} - N_v)]^{1/2}$.

Crystallographic Studies of Fe(saloph)catH and $[Fe(salen)]_2hq$. Crystals of both compounds were cleaved to give parallelepipeds that were sealed in glass capillaries under nitrogen atmosphere. Preliminary Weissenberg and oscillation photographs showed triclinic symmetry for Fe(saloph)catH and orthorhombic symmetry for $[Fe(salen)]_2hq$. Accurate lattice constants for the two compounds were determined from least-squares fits of 15 moderate angle diffractometer measured reflections and are given in Table I. The two data sets were collected on a computer-controlled four-circle Syntex $P2_1$ diffractometer using a variable speed 1° ω scan and graphite-monochromated radiation. Cu K$\bar{\alpha}$ X-rays were used with Fe(saloph)catH to compensate for small crystal size while Mo K$\bar{\alpha}$ X-rays were used for $[Fe(salen)]_2hq$.

Fe(saloph)catH was assumed to belong to the space group $P\bar{1}$ because density measurements showed two molecules per unit cell; the successful structure refinement vindicated this choice. Systematic absences for $[Fe(salen)]_2hq$ uniquely fit *Pbca*. Unsharpened Patterson

(7) Felton, R. H.; Cheung, L. D.; Phillips, R. S.; May, S. W. *Biochem. Biophys. Res. Commun.* **1978**, *85*, 844–850.
(8) Que, L., Jr.; Heistand, R. H., II *J. Am. Chem. Soc.* **1979**, *101*, 2219–2221.
(9) Que, L., Jr.; Lipscomb, J. D.; Munck, E.; Wood, J. M. *Biochim. Biophys. Acta* **1977**, *485*, 60–74.
(10) Raymond, K. N.; Isied, S. S.; Brown, L. D.; Fronczek, F. F.; Nibert, J. H. *J. Am. Chem. Soc.* **1976**, *98*, 1767–1774. Anderson, B. F.; Buckingham, D. A.; Robertson, G. B.; Webb, J., Murray, K. S.; Clark, P. E. *Nature (London)* **1976**, *262*, 722–724.
(11) Lauffer, R. B.; Heistand, R. H., II; Que, L., Jr. *J. Am. Chem. Soc.* **1981**, *103*, 3947–3949.
(12) Abbreviations used: saloph, *N,N'*-(1,2-phenylene)bis(salicylidenimine) dianion; $catH_2$, catechol; salen, *N,N'*-ethylenebis(salicylidenimine) dianion; hqH_2, hydroquinone; OAc, acetate; EHPG, ethylenebis(*o*-hydroxyphenylglycine) tetraanion; $TPPH_2$, *meso*-tetraphenylporphin; salps, *N,N'*-(2,2'-diphenyl disulfide)bis(salicylidenimine) dianion; sal, salicylidenimine anion; $DBcatH_2$, 3,5-di-*tert*-butylcatechol.
(13) Floriani, C.; Fachinetti, G.; Calderazzo, F. *J. Chem. Soc., Dalton Trans.* **1973**, 765–769.
(14) Kessel, S. L.; Hendrickson, D. N. *Inorg. Chem.* **1978**, *17*, 2630–2635.
(15) Koch, S.; Holm, R. H.; Frankel, R. B. *J. Am. Chem. Soc.* **1975**, *97*, 6714–6723.
(16) Lewis, J.; Mabbs, F. E.; Richards, A.; Thornley, A. S. *J. Chem. Soc. A* **1969**, 1993–1997.

Table II. Atomic Fractional Coordinates for Fe(saloph)catH[a]

atom	x	y	z
Fe	0.3936 (1)	0.3279 (1)	0.2022 (1)
O1	0.3539 (5)	0.2370 (6)	0.3152 (3)
O2	0.2917 (5)	0.1972 (5)	0.1249 (3)
O3	0.2969 (5)	0.5596 (5)	0.2030 (3)
O4	0.2822 (6)	0.8906 (5)	0.1891 (3)
N1	0.5865 (6)	0.3315 (6)	0.2677 (4)
N2	0.5258 (5)	0.2933 (6)	0.0829 (4)
C1	0.4031 (8)	0.2418 (8)	0.4048 (4)
C2	0.3273 (9)	0.2081 (11)	0.4802 (5)
C3	0.3754 (10)	0.2116 (10)	0.5741 (5)
C4	0.5028 (9)	0.2419 (10)	0.5981 (5)
C5	0.5785 (8)	0.2733 (9)	0.5251 (5)
C6	0.5335 (7)	0.2754 (8)	0.4288 (4)
C7	0.6177 (7)	0.3134 (8)	0.3569 (5)
C8	0.6826 (7)	0.3646 (7)	0.2037 (5)
C9	0.8006 (7)	0.4155 (9)	0.2310 (5)
C10	0.8850 (8)	0.4420 (10)	0.1615 (6)
C11	0.8563 (7)	0.4158 (9)	0.0638 (5)
C12	0.7383 (7)	0.3691 (8)	0.0352 (5)
C13	0.6505 (6)	0.3426 (7)	0.1051 (4)
C14	0.5006 (6)	0.2398 (7)	−0.0056 (4)
C15	0.3812 (7)	0.1856 (7)	−0.0362 (4)
C16	0.3652 (7)	0.1448 (8)	−0.1355 (5)
C17	0.2538 (9)	0.0914 (9)	−0.1726 (5)
C18	0.1569 (8)	0.0738 (8)	−0.1080 (5)
C19	0.1684 (7)	0.1074 (8)	−0.0098 (5)
C20	0.2810 (7)	0.1659 (7)	0.0300 (4)
C21	0.2022 (7)	0.6842 (8)	0.2594 (4)
C22	0.1925 (7)	0.8616 (8)	0.2526 (4)
C23	0.0962 (9)	0.9911 (9)	0.3070 (5)
C24	0.0088 (9)	0.9495 (12)	0.3710 (6)
C25	0.0196 (8)	0.7797 (13)	0.3803 (6)
C26	0.1155 (8)	0.6460 (10)	0.3254 (5)
H(O4)	0.250 (9)	0.993 (12)	0.183 (6)
H2	0.232 (11)	0.208 (12)	0.463 (7)
H3	0.341 (11)	0.188 (13)	0.620 (8)
H4	0.537 (10)	0.249 (12)	0.661 (8)
H5	0.659 (11)	0.278 (12)	0.539 (7)
H7	0.700 (10)	0.310 (10)	0.380 (6)
H9	0.826 (9)	0.422 (11)	0.296 (7)
H10	0.965 (12)	0.446 (12)	0.181 (7)
H11	0.908 (10)	0.426 (11)	0.017 (7)
H12	0.728 (9)	0.356 (10)	−0.027 (7)
H14	0.567 (9)	0.234 (10)	−0.049 (6)
H16	0.432 (9)	0.145 (10)	−0.177 (6)
H17	0.248 (9)	0.069 (11)	−0.250 (7)
H18	0.081 (10)	0.045 (10)	−0.134 (6)
H19	0.108 (9)	0.095 (10)	0.037 (6)
H23	0.088 (9)	0.123 (12)	0.295 (6)
H24	0.944 (11)	0.037 (13)	0.406 (7)
H25	0.981 (11)	0.738 (12)	0.430 (7)
H26	0.134 (9)	0.512 (12)	0.337 (6)

[a] Estimated standard deviations of the last significant digits are in parentheses.

syntheses gave the iron positions in the two compounds. Subsequent refinement and F_o syntheses gave the positions of all remaining nonhydrogen atoms. After further refinement and compensation for anomalous scattering by iron, ΔF maps gave the positions of all hydrogen atoms. The hydrogen positions were refined with fixed isotropic temperature factors while anisotropic factors were used for all nonhydrogen atoms. All least-squares refinements were limited to diagonal elements until the final stages, when the matrices were blocked off as salicylyl, diamine, and benzenediol moieties. A weighting scheme using $1/\sigma_I$ was used in the refinements, and estimated standard deviations were obtained from BOND.[17] No absorption corrections were applied, and this may account for the somewhat lower accuracy of the Fe(saloph)catH structure.

(17) Computer programs used for the analyses were as follows: XRAY76, the X-ray system of crystallographic programs (Stewart, J. M., Ed. University of Maryland, Technical Report TR-445, March 1976); ORTEP, crystallographic illustration program (Johnson, C. K., Oak Ridge ORNL-3794); BOND, structural parameters and errors (Hirotsu, K., Cornell University, 1978).

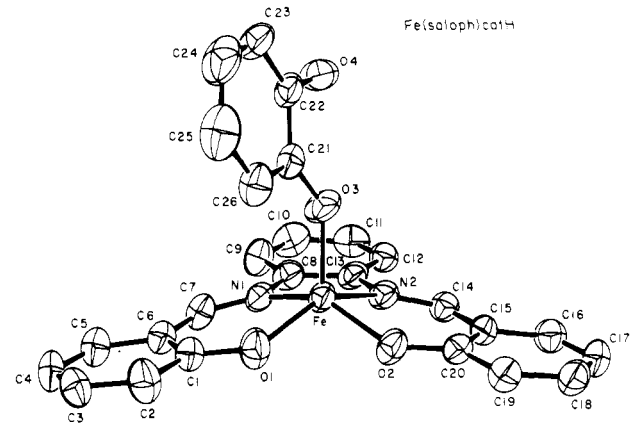

Figure 2. Structure and labeling of Fe(saloph)catH. Thermal ellipsoids represent the 50% probability surfaces.

Table IV. Selected Structural Parameters

Bond Lengths (Å)

	Fe(saloph)catH		
Fe-O1	1.897 (5)	N2-C13	1.432 (8)
Fe-O2	1.912 (5)	N2-C14	1.302 (8)
Fe-O3	1.828 (4)	C1-C6	1.429 (11)
Fe-N1	2.104 (6)	C6-C7	1.438 (10)
Fe-N2	2.090 (6)	C8-C13	1.398 (9)
O1-C1	1.320 (7)	C14-C15	1.426 (10)
O2-C20	1.321 (7)	C15-C20	1.431 (10)
O3-C21	1.352 (7)	O2-H(O4)	2.07 (9)
N1-C7	1.275 (9)	O4-C22	1.360 (9)
N1-C8	1.427 (10)	O4-H(O4)	0.81 (9)
	$[Fe(salen)]_2hq$		
Fe-O1	1.898 (2)	N2-C9	1.467 (4)
Fe-O2	1.912 (2)	N2-C10	1.289 (3)
Fe-O3	1.861 (2)	C1-C6	1.408 (5)
Fe-N1	2.089 (3)	C6-C7	1.439 (4)
Fe-N2	2.103 (2)	C8-C9	1.508 (5)
O1-C1	1.318 (4)	C10-C11	1.440 (4)
O2-C16	1.318 (3)	C11-C16	1.412 (3)
O3-C17	1.349 (3)	C17-C18	1.399 (3)
N1-C7	1.280 (3)	C17-C19	1.392 (3)
N1-C8	1.470 (4)	C18-C19′	1.378 (4)

Bond Angles (Deg)

	Fe(saloph)catH		
O1-Fe-O2	90.1 (2)	Fe-O2-C20	131.8 (5)
O1-Fe-O3	110.9 (2)	Fe-O3-C21	138.5 (4)
O1-Fe-N1	87.5 (2)	Fe-N1-C7	125.3 (5)
O1-Fe-N2	147.2 (2)	Fe-N1-C8	113.9 (4)
O2-Fe-O3	108.9 (2)	C7-N1-C8	120.8 (6)
O2-Fe-N1	147.3 (2)	Fe-N2-C13	113.6 (4)
O2-Fe-N2	87.5 (2)	Fe-N2-C14	125.9 (4)
O3-Fe-N1	102.4 (2)	C13-N2-C14	120.4 (5)
O3-Fe-N2	100.8 (2)	O2-H(O4)-O4	142 (7)
N1-Fe-N2	77.3 (2)	C22-O4-H(O4)	103 (7)
Fe-O1-C1	132.1 (5)		
	$[Fe(salen)]_2hq$		
O1-Fe-O2	95.1 (1)	Fe-O1-C1	133.5 (2)
O1-Fe-O3	114.2 (1)	Fe-O2-C16	128.8 (2)
O1-Fe-N1	87.1 (1)	Fe-O3-C17	132.1 (2)
O1-Fe-N2	144.1 (1)	Fe-N1-C7	128.0 (2)
O2-Fe-O3	104.5 (1)	Fe-N1-C8	112.0 (2)
O2-Fe-N1	154.2 (1)	C7-N1-C8	120.0 (3)
O2-Fe-N2	86.2 (1)	Fe-N2-C9	116.0 (2)
O3-Fe-N1	97.9 (1)	Fe-N2-C10	123.2 (2)
O3-Fe-N2	100.0 (1)	C9-N2-C10	119.9 (3)
N1-Fe-N2	77.4 (1)		

Results

Fe(saloph)catH crystallizes in the monoclinic space group $P\bar{1}$ with a unit cell consisting of two square-pyramidal molecules related by a center of inversion (Figure 1). The numbering scheme for the molecule is shown in Figure 2; atomic

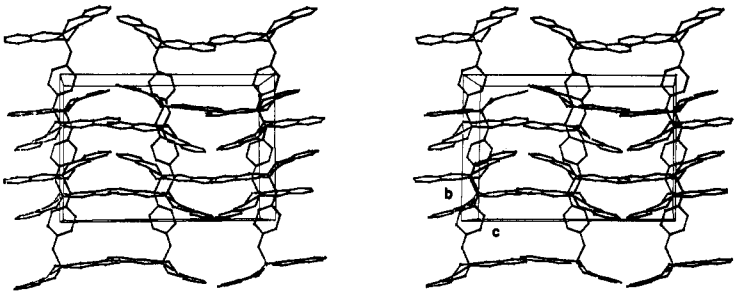

Figure 3. Packing diagram of $[Fe(salen)]_2hq$ viewed down the *a* axis. The top four dimers in the *bc* plane have been omitted for clarity.

Table VIII. Bond Distance Changes vs. Free salophH$_2$[a]

	$\Delta(C_1-O)$	$\Delta(C_6-C_7)$	$\Delta(C_7-N)$
Co	−0.047	−0.037	+0.029
Cu	−0.046	−0.028	+0.009
Fe	−0.025	−0.017	+0.001

[a] Data for ref 24 and 25 and this work.

coordinates, thermal parameters, selected bond distances and bond angles, and structure factors are found in Tables II–V, respectively. Complete lists of bond lengths and angles are reported in Tables VI and VII, respectively. The square-pyramidal coordination geometry around the iron is shown clearly by the ORTEP drawing in Figure 2. The atoms N1, O1, O2, and N2 are essentially coplanar, and the iron is raised 0.55 Å above this plane. The catecholate oxygen O3 is at the apex of the pyramid, 2.37 Å above the base, 0.04 Å off center, with an Fe–O3–C21 angle of 138.5 (4)°. The Fe–O3 bond distance, 1.828 (4) Å, is shorter than the equatorial Fe–O1, O2 bonds (average 1.905 (5) Å). As expected the Fe–N1, N2 distances (average 2.097 (5) Å) are longer than the Fe–O1, O2 bonds.

The saloph ligand has the "umbrella" shape,[18] similar to that of the μ-oxo-bridged dimers[19-22] and the monomeric iron salen chloride.[23] For salen, this conformation is characterized by the dihedral angles the salicylyl phenyl rings make with the NOON plane (α and β) and by the angle the two rings make with each other (γ) where $\alpha = \beta = \gamma = 0$ is a planar conformation and $\alpha + \beta \simeq \gamma$ is umbrella conformation.[18] Similar angles can be defined for the saloph conformation, in addition to a fourth angle (δ) which defines the angular relationship of the phenylene ring to the NOON plane. The values of α, β, γ, and δ for Fe(saloph)catH are 8.0, 7.0, 13.8, and 1.6, respectively. By comparison to Fe(salen)X complexes with umbrella conformations, where γ ranges from 11 to 41° (average 24.6°),[18] the saloph in Fe(saloph)catH is quite planar. The greater planarity of the saloph ligand can be attributed to the π delocalization on the ligand upon metal coordination and is reflected in changes of bond distances in going from free ligand to metal complex. Table VIII shows a comparison of relevant bond distances in Fe(saloph)catH, Co(saloph),[24] and Cu(saloph)[25] with the free ligand, indicating that delocalization is somewhat less significant in the iron complex than in the cobalt and copper complexes.

Table IX. Atomic Fractional Coordinates for $[Fe(salen)_2hq$

atom	*x*	*y*	*z*
Fe	0.5251 (0)	0.1755 (0)	0.5020 (0)
O1	0.5635 (2)	0.1700 (2)	0.4079 (1)
O2	0.6403 (1)	0.0969 (2)	0.5338 (1)
O3	0.5429 (1)	0.3030 (1)	0.5426 (1)
N1	0.3728 (2)	0.1952 (2)	0.4685 (1)
N2	0.4390 (2)	0.1020 (2)	0.5793 (1)
C1	0.5138 (3)	0.1892 (2)	0.3500 (2)
C2	0.5694 (4)	0.1876 (3)	0.2882 (2)
C3	0.5214 (4)	0.2039 (3)	0.2259 (2)
C4	0.4160 (4)	0.2237 (3)	0.2231 (2)
C5	0.3601 (4)	0.2271 (3)	0.2827 (2)
C6	0.4069 (3)	0.2097 (2)	0.3474 (2)
C7	0.3406 (2)	0.2084 (2)	0.4068 (1)
C8	0.2986 (2)	0.1936 (3)	0.5258 (2)
C9	0.3261 (2)	0.1042 (3)	0.5711 (2)
C10	0.4791 (2)	0.0705 (2)	0.6362 (1)
C11	0.5883 (2)	0.0600 (2)	0.6496 (1)
C12	0.6190 (3)	0.0328 (3)	0.7165 (2)
C13	0.7217 (3)	0.0155 (3)	0.7318 (2)
C14	0.7948 (3)	0.0200 (3)	0.6787 (2)
C15	0.7668 (3)	0.0461 (3)	0.6134 (2)
C16	0.6633 (2)	0.0688 (2)	0.5971 (1)
C17	0.5207 (2)	0.3983 (2)	0.5208 (1)
C18	0.5444 (2)	0.4324 (2)	0.4544 (1)
C19	0.4753 (2)	0.4684 (2)	0.5653 (1)
H2	0.637 (4)	0.174 (4)	0.292 (3)
H3	0.565 (4)	0.212 (4)	0.185 (3)
H4	0.391 (4)	0.228 (4)	0.174 (3)
H5	0.288 (4)	0.244 (4)	0.282 (3)
H7	0.270 (4)	0.220 (3)	0.399 (2)
H8a	0.231 (5)	0.190 (4)	0.508 (2)
H8b	0.309 (4)	0.258 (4)	0.554 (2)
H9a	0.305 (4)	0.043 (4)	0.550 (2)
H9b	0.302 (4)	0.114 (4)	0.616 (2)
H10	0.428 (4)	0.048 (3)	0.673 (2)
H12	0.560 (4)	0.034 (3)	0.754 (3)
H13	0.737 (4)	−0.006 (4)	0.781 (3)
H14	0.871 (4)	0.001 (3)	0.691 (3)
H15	0.816 (4)	0.056 (4)	0.577 (2)
H18	0.569 (3)	0.386 (3)	0.426 (2)
H19	0.460 (3)	0.453 (3)	0.615 (2)

The coordinated catecholate is clearly not chelated to the iron. It is raised like a flag, tilted 15.1° from the perpendicular, and angled approximately 25° from the ideal vertical mirror plane. The uncoordinated oxygen (O4) is 4.373 (4) Å from the iron within the molecule and 4.013 (4) Å from the iron in the molecule translated one unit along the *y* axis; however, it is within hydrogen-bonding distance of the salicylyl hydroxyl O2 in the translated molecule. The distance of 2.751 (6) Å indicates an even stronger bond than those in the crystalline catechol[26] itself, which are 2.795 Å and 2.806 Å. A hydrogen, H(O4), was located in an electron density difference map and refined isotropically to a position 0.81 (9) Å from O4 and 2.07 (9) Å from O2′. The H(O4)–O4–C22

(18) Calligaris, M.; Nardin, G.; Randaccio, L. *Coord. Chem. Rev.* **1972**, *7*, 385–403.
(19) Gerloch, M.; McKenzie, E. D.; Towl, A. D. C. *J. Chem. Soc. A* **1969**, 2850–2858.
(20) Atoomyan, L. O.; D'yachenko, O. A.; Soboleva, S. V. *Zh. Struckt. Khim.* **1970**, *11*, 557–558.
(21) Coggon, P.; McPhail, A. T.; Mabbs, F. E.; McLachlan, V. N. *J. Chem. Soc. A* **1971**, 1014–1019.
(22) Davies, J. E.; Gatehouse, B. M. *Acta Crystallogr., Sect. B* **1973**, *B29*, 1934–1942.
(23) Gerloch, M.; Mabbs, F. E. *J. Chem. Soc. A* **1967**, 1598–1608.
(24) Pahor, N. B.; Calligaris, M.; Delise, P.; Dodic, G.; Nardin, G.; Randaccio, L. *J. Chem. Soc., Dalton Trans.* **1976**, 2478–2483.
(25) Cassoux, P.; Gleizes, A. *Inorg. Chem.* **1980**, *19*, 665–672.
(26) Brown, C. J. *Acta Crystallogr.* **1966**, *21*, 170–174.

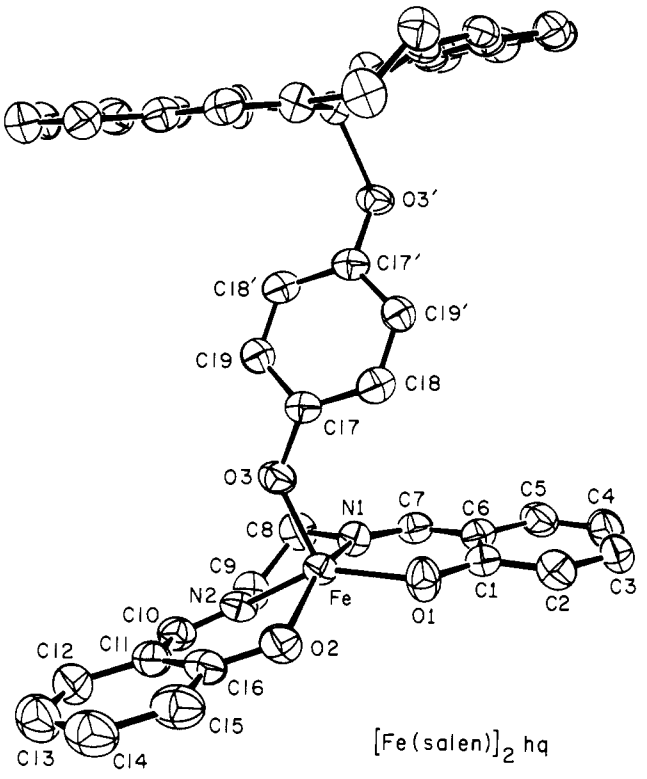

Figure 4. Structure and labeling of $[Fe(salen)]_2hq$. Thermal ellipsoids represent the 50% probability surfaces.

angle is 103 (7)°, and the O4–H(O4)–O2 angle is 142 (7)°. Although there is a large uncertainty in the position of the hydrogen, the bond lengths and angles obtained are normal for a hydrogen bond. This interaction is shown by dashed lines in the stereoview of the unit cell of Figure 1. Confirmation of the hydrogen bond is found in the infrared spectrum of Fe(saloph)catH.[27] Catecholate structural parameters in this molecule are comparable to those of other metal catecholate complexes.[10,28]

$[Fe(salen)]_2hq$ crystallizes in the orthorhombic space group *Pbca* with the crystallographic inversion center in the center of the hydroquinone moiety that bridges the two iron salen species (Figure 3). The numbering scheme for the molecule is shown in Figure 4, with atomic coordinates, thermal parameters, selected bond distances and bond angles, and structure factors found in Tables IX, X, IV, and XI, respectively. Complete lists of bond lengths and angles can be found in Tables XII and XIII, respectively. The ORTEP drawing in Figure 4 shows the stepped square-pyramidal geometry. The N1,O1,O2,N2 plane shows an average deviation of 0.093 Å and a torsional angle of 8.0°; the iron is 0.50 Å above this plane. The hydroquinone oxygen (O3) is at the apex of the pyramid, 2.35 Å above the base and 0.07 Å off center, with an Fe–O3–C17 angle of 132.1 (2)°. The Fe–O3 bond distance, 1.861 (2) Å, is again shorter than the equatorial Fe–O1, O2 bonds (average 1.905 (5) Å). which are shorter than the Fe–N1, N2 bonds (average 2.096 (5) Å).

The salen ligand adopts a stepped conformation ($\alpha + \gamma \simeq \beta$)[18] where values for α, β, and γ are 8.8, 15.5, and 8.0°, respectively. The only other iron salen complex with this conformation is the dimeric $[Fe(salen)Cl]_2$,[29] where the iron is hexacoordinate. We suggest that intermolecular stacking forces between tetradentate ligands (Figure 3) determine this conformation.

The hydroquinone bridges the two iron atoms symmetrically. Compared to Fe(saloph)catH, the hydroquinone plane is considerably more tilted with respect to NOON plane, 56°. As expected, the C–O bond is shorter (1.349 (3) Å) than the C–O bond in free hydroquinone (average of five structures 1.398; σ 0.010 Å)[30]. Otherwise, there are no other noticeable structural deviations in the hydroquinone compared with the free species. No intermolecular Fe–heteroatom interactions are observed; thus, the structure is consistent with the proposed antiferromagnetic exchange between the ferric centers via the hydroquinone bridge.[14]

Discussion

Fe(saloph)catH and $[Fe(salen)]_2hq$ represent the first monodentate catecholate and the first bridged hydroquinone[31] structures, respectively, in the literature. There is a paucity of unconstrained transition-metal phenolate structures, probably due to the lability of these compounds. Such problems were circumvented in the two complexes by using charged iron fragments to bind the phenolates, thus forming neutral complexes, and by taking advantage of the chelate effect inherent in the tetradentate ligands to fill the remaining coordination sites.

The two structures are rather similar, with the main distinction being that one is mononuclear and the other binuclear. The average Fe–O and Fe–N bond lengths are the same in both structures, 1.905 and 2.079 Å, respectively, and are in excellent agreement with the average Fe–O and Fe–N bond distances (1.915 (5) and 2.091 (6) Å, respectively) of the corresponding bonds in the three $[Fe(salen)]_2O$ structures[19-22] and the monomeric Fe(salen)Cl complex.[23]

As expected for high-spin ferric complexes with square-pyramidal geometry, the iron in both complexes is raised above the basal mean plane: 0.55 Å for Fe(saloph)catH and 0.50 Å for $[Fe(salen)]_2hq$. These displacements fall within the range of 0.49–0.58 Å found for other iron complexes of similar geometry.[18] Also expected for square-pyramidal coordination is the shortening of the apical Fe–O bond: 1.828 (4) Å for Fe(saloph)catH and 1.861 (2) Å for $[Fe(salen)]_2hq$ compared to 2.015 (6) Å for $[Fe(cat)_3]^{3-}$[10] and 1.906 (5) Å for $[Fe(EHPG)]^-$,[33] both octahedral complexes. For comparison, the apical Fe–Cl bond distance in Fe(salen)Cl is 2.238 (4) Å;[23] this lengthens to 2.294 (3) Å in the dimeric $[Fe(salen)Cl]_2$[29] and 2.314 (4) Å in the octahedral Fe(salps)Cl.[34] The apical Fe–O bond for Fe(saloph)catH is significantly shorter than that for $[Fe(salen)]_2hq$, suggesting a stronger interaction for the catecholate ligand. Such an interaction is also reflected in our solution studies by the more favorable formation constant for the catecholate complex.[27]

The apical iron–oxygen–phenolate bond angle is another interesting structural feature of these complexes. This angle is 138.5 (4)° for Fe(saloph)catH and 132.1 (2)° for $[Fe(salen)]_2hq$ (135° for FeTPPcatH[35]); it exhibits little dependence on the basal ligand, the type of phenolate, and the phenolate conformation relative to the Fe–O bond or the basal

(27) Heistand, R. H. II; Lauffer, R. B.; Fikrig, E.; Que, L., Jr. *J. Am. Chem. Soc.*, in press.
(28) Kobayashi, A.; Ito, T.; Marumo, F.; Saito, Y. *Acta Crystallogr. Sect. B* **1972**, *B28*, 3446–3451. Allcock, H. R.; Bissell, E. C. *J. Am. Chem. Soc.* **1973**, *95*, 3154–3157. Flynn, J. J.; Boer, F. P. *Ibid.* **1969**, *91*, 5756–5761.
(29) Gerloch, M.; Mabbs, F. E. *J. Chem. Soc. A* **1967**, 1900–1908.
(30) Wyckoff, R. W. G. "Crystal Structures"; Wiley-Interscience: New York, 1963; Vol. 6, Part 1, pp 204–208.
(31) The structure of a bridging 3,6-dichloro-2,5-dihydroxy-1,4-benzoquinone complex has been reported.[32] This ligand can be considered a hydroquinone, albeit a highly specialized one, with substituents which allow it to act as a bridging tetradentate ligand.
(32) Pierpont, C. G.; Francesconi, L. C.; Hendrickson, D. N. *Inorg. Chem.* **1977**, *16*, 2367–2376.
(33) Bailey, N. A.; Cummins, D.; McKenzie, E. D.; Worthington, J. M. *Inorg. Chim. Acta* **1981**, *50*, 111–120.
(34) Bertrand, J. A.; Breece, J. L. *Inorg. Chim. Acta* **1974**, *8*, 267–272.
(35) Rogers, M. E.; Que, L., Jr., unpublished observations.

plane. The Fe–O–C_{Ph}–C_{Ph} torsional angles of 157 and 137° for Fe(saloph)catH and $[Fe(salen)]_2hq$, respectively, show that rotation about the phenolate C–O bond is not restrained. Furthermore, the projection of the C–O bond of the axial ligand onto the basal plane is colinear with the Fe–O1 bond in Fe(saloph)catH, while the corresponding bond in $[Fe(salen)]_2hq$ bisects the O1–Fe–N1 angle. These factors, however, do not appear to affect the iron–oxygen–phenolate bond angle significantly.

These angles can be compared to those found in μ-oxo iron dimers. The title complexes may be considered similar to the dimers by the substitution of an aryl group for the FeL moiety. The $[Fe(salen)]_2O$ structures exhibit an Fe–O–Fe angle of 139–144°,[19-22] while the four porphyrin μ-oxo structures exhibit angles ranging from 161.1 to 178.5°.[36,37] The disparity in these angles has stimulated discussion on whether the Fe–O–Fe angle is ideally linear or bent.[38] Recent extended Hückel calculations[39] indicate a preference for the bent configuration with a rather shallow minimum on the energy surface occurring near 140°. Thus, the porphyrin μ-oxo dimers have near linear configurations in order to minimize nonbonding interactions. Similarly, the bulkier $[Fe(sal\text{-}N\text{-}n\text{-}C_3H_7)_2]_2O$,[40] $[Fe(sal\text{-}N\text{-}C_6H_4\text{-}p\text{-}Cl)_2]_2O$,[40] and $[[Fe(HEDTA)]_2O]^{2-}$[41] have Fe–O–Fe angles closer to linear than those for $[Fe(salen)]_2O$. Indeed, the Fe–O–Fe angles in the $[Fe(salen)]_2O$ complexes as well as the Fe–O–phenolate angles in the title complexes all approximate the theoretically predicted ideal angle, suggesting that the factors affecting geometry in these complexes may be rather similar.

Our two structures pose yet another puzzling question—why two such similar ligands give rise to complexes of different metal-to-ligand stoichiometries. The catecholate complex is mononuclear while the hydroquinone complex is binuclear. There is clearly no steric constraint which prevents the coordination of a second Fe(saloph) moiety onto the uncoordinated catecholate oxygen. Indeed, Hendrickson has reported such a binuclear complex with Fe(salen) and tetrachlorocatecholate as the bridging ligand.[42] It may be argued that the proton on Fe(saloph)catH is not acidic enough to be replaced by $Fe(saloph)^+$; however, similar arguments should apply to the hydroquinone complex, yet a binuclear complex is formed in the latter case. A similar situation occurs with FeTPP complexes. Hendrickson has synthesized binuclear complexes with hydroquinone and tetrachlorocatecholate ligands,[43] while we have prepared and crystallized a mononuclear FeTPPcatH.[35] Solution studies on Fe(saloph)catH as well as Fe(salen)catH show that these complexes are mononuclear, i.e., they exhibit a 1:1 metal ligand stoichiometry.[27] Our studies also show that the complex of hydroquinone and Fe(salen) is mononuclear in solution.[27] The balance of the Fe(salen) is in the form of the μ-oxo dimer which can be dissociated by the addition of excess hydroquinone. Interestingly enough, our synthesis of the hydroquinone complex uses a 50-fold excess of ligand over Fe(salen)OAc, an excess sufficient to form the mononuclear complex completely in solution; however, it is the dimer which crystallizes. It would thus appear that the formation of the binuclear complex is favored by the crystallization process.

In summary, we have determined the crystallographic structures of the iron complexes of two important redox active ligands. Fe(saloph)catH is the first iron monodentate catecholate structure reported and serves as a model for a proposed dioxygenase–substrate complex. We have already demonstrated that the closely related Fe(salen)DBcatH reacts readily with oxygen in accordance to our proposed mechanism.[11] Such studies are continuing.

Acknowledgment. We are most grateful to Professor Jon Clardy for his invaluable assistance and encouragement. This work was supported by National Institutes of Health Grant GM-25422. R.H.H. is a National Institutes of Health Predoctoral Trainee (GM 07273, 1978–1981).

Registry No. Fe(saloph)catH, 80041-63-0; $[Fe(salen)]_2hq$, 41180-62-5; Fe(saloph)OAc, 24844-43-7; Fe(salen)OAc, 41742-84-1.

Supplementary Material Available: Tables III and V–VII listing anisotropic thermal parameters, structure factors, bond lengths, and bond angles, respectively, for Fe(saloph)catH, and Tables X–XIII listing anisotropic thermal parameters, structure factors, bond lengths, and bond angles, respectively, for $[Fe(salen)]_2hq$ (30 pages). Ordering information is given on any current masthead page.

(36) Landrum, J. T.; Grimmett, D.; Haller, K. J.; Scheidt, W. R.; Reed, C. A. *J. Am. Chem. Soc.* **1981**, *103*, 2640–2650.
(37) Hoffman, A. B.; Collins, C. M.; Day, V. W.; Fleischer, E. B.; Srivastava, T. S.; Hoard, J. L. *J. Am. Chem. Soc.* **1972**, *94*, 3620–3626.
(38) Murray, K. S. *Coord. Chem. Rev.* **1974**, *12*, 1–35.
(39) Tatsumi, K.; Hoffmann, R. *J. Am. Chem. Soc.* **1981**, *103*, 3328–3341.
(40) Davies, J. E.; Gatehouse, B. M. *Cryst. Struct. Commun.* **1972**, *1*, 115–120.
(41) Lippard, S. J.; Schugar, H. J.; Walling, C. *Inorg. Chem.* **1967**, *6*, 1825–1831.
(42) Kessel, S. L.; Emberson, R. M.; Debrunner, P. G.; Hendrickson, D. N. *Inorg. Chem.* **1980**, *19*, 1170–1178.
(43) Kessel, S. L.; Hendrickson, D. N. *Inorg. Chem.* **1980**, *19*, 1883–1889.